PROCEEDINGS OF SCIENCE

Study of Global Temperature Fluctuations in pp collisions at LHC energies

E. Loza[*1], **I. Bautista**[2], **E. De la Fuente**[1]

[1]*Departmento de Física, CUCEI, Universidad de Guadalajara, Mexico.*
[2]*Facultad de Ciencias Físico Matemáticas, Benemérita Universidad Autónoma de Puebla, 1152, Mexico.*
Email: edgar.loza@alumnos.udg.mx, irais.bautista.guzman@cern.ch, edfuente@gmail.com

Under the extreme conditions of ultrarelativistic pp collisions, free gluons and quarks can form a state of matter called the Quark-Gluon-Plasma. String Percolation Theory can describe quantitatively the phase transition that forms the collectivity. Within the model strings are representations of the interactions between quarks and they form clusters that reach a critical density that suggests the formation of QGP. In this work we study the Global Temperatures assigned to pp collisions at center-of-mass energies $\sqrt{s}$ = 0.9, 2.76, 7 and 13 TeV for several multiplicity classes. We found the universal behavior of Global Temperatures as the multiplicity increases, regardless of the center-of-mass energy of the collision.

7th Annual Conference on Large Hadron Collider Physics - LHCP2019
20-25 May, 2019
Puebla, Mexico

*Speaker.

PoS(LHCP2019)053

1. Introduction

The Quark-Gluon-Plasma (QGP) is a matter state where quarks and gluons are "free". The QCP is reached as the hadron density increases, quarks start to find themselves very near each other. At some point, it is impossible to know which quark corresponds to which hadron. Defining a hadron has no longer sense and it is possible to talk about unbounded quarks. This is a special state since quarks are supposed to be always together (confined matter). Through increments of temperature T and baryochemical potential more and more quarks become unconfined. In statistical mechanics, the matter is a system of many constituents in local thermal equilibrium, characterized by several global quantities (state variables). For different values of the state variables, the system changes its properties. Therefore, there exist phase transitions occurring when the system changes from one state to the other [1].

2. String Percolation Theory

Percolation theory is a model to describe phase transitions. The basic idea consists of an n-dimensional lattice, of size L, whose sites have a probability p of being occupied. Randomly, occupied sites get together. These groups are known as clusters. Percolation theory deals with these formed clusters properties [2].

When a critical density is reached, a cluster appears spanning the whole system and the so-called Percolation Density Parameter ζ characterizes such cluster. During the cluster formation, the objects occupying sites lose their independence, for they form clusters. In ultrarelativistic collisions, color strings are these objects. They can be seen as small discs on the collision transverse plane. Strings are filled with a certain color field. As the energy and number of colliding nuclei increase, more strings appear and form clusters. The increment in the string number causes a density augmentation until it reaches a critical point. Here the phase transition takes place [3].

In String Percolation Model (SPM), a color string cluster is a prerequisite for the formation of QGP. Therefore, consider the transverse collision plane surface S, and N_p^s small discs randomly distributed over S. The discs can overlap and have an area $s = \pi r_0^2$ and let $S = \pi R^2$. The percolation density parameter or transverse impact parameter density that describes this cluster, when formed, is given by [3]

$$\zeta = \frac{\pi r_0^2}{\pi R^2} N_p^s = \left(\frac{r_0}{R_p}\right)^2 N_p^s \tag{2.1}$$

where $r_0 \approx 0.25$ fm is the transverse size of a string, $R_p \approx 1$ fm is the proton transverse size and N^s is the average number of strings [4]. The string average number depends on the center-of-mass energy $\sqrt{s}$. In pp collisions, the average string number is given by [4]

$$N_p^s = 2 + 4\left(\frac{r_0}{R_p}\right)^2 \left(\frac{\sqrt{s}}{m_p}\right)^{2\lambda}, \tag{2.2}$$

where m_p is the proton mass and $\lambda \approx 0.201$ is a parameter obtained from fitting data. Another important parameter is the Color Suppression Factor [5]

$$F(\zeta) = \sqrt{\frac{1-e^{-\zeta}}{\zeta}}, \tag{2.3}$$

which defines the geometric scaling function of the system and it relates the string multiplicity to the string interaction value [6]. The string tension varies because of the chromo-electric field variations. Such changes result in thermal fluctuations [7]. Therefore, the temperature is related to the string tension and the Color Suppression Factor by [6]

$$T(\zeta) = \sqrt{\frac{\langle p_T^2 \rangle_1}{2F(\zeta)}}. \tag{2.4}$$

Here $\langle p_T^2 \rangle$ is the single string average transverse momentum, whose value is $\sqrt{\langle p_T^2 \rangle}$ = 190.25 MeV [7].

2.1 Momentum distributions

Transverse momentum spectra from different particles produced in pp collisions at different $\sqrt{s}$ were measured by the CMS [8, 9]. By fitting the data we obtain valuable information regarding the collision's thermal distribution. To obtain the value of ζ from data, the parametrizations

$$\frac{dN}{dp_T^2} = \frac{a}{(p_0+p_T)^\alpha} \tag{2.5a}$$

$$\frac{1}{N}\frac{d^2N}{d\eta\, dp_T} = \frac{a p_0^{\alpha-2}}{(p_0+p_T)^{\alpha-1}}, \tag{2.5b}$$

are used to compute the p_T distribution [6, 7]. The parameters a, p_0, α are found from fitting p_T distributions [10]. The p_T distributions for nucleus-nucleus collision require modification due to the strings interactions [11]

$$\frac{dN}{dp_T^2} = \frac{a'}{\left(p_0\sqrt{\frac{F(\zeta_{pp})}{F(\zeta_{HM})}}+p_T\right)^\alpha} \tag{2.6a}$$

$$\frac{1}{N}\frac{d^2N}{d\eta\, dp_T} = \frac{a'(p_0\sqrt{\frac{F(\zeta_{pp})}{F(\zeta_{HM})}})^{\alpha-2}}{\left(p_0\sqrt{\frac{F(\zeta_{pp})}{F(\zeta_{HM})}}+p_T\right)^{\alpha-1}}, \tag{2.6b}$$

where ζ_{pp} is the transverse impact color string density calculated from (2.1), (2.2) and (2.3) and depends on $\sqrt{s}$ and ζ_{HM} is the high multiplicity color string density obtained from high multiplicity data.

3. Methodology

Momentum spectra data from pp collisions at LHC energies of $\sqrt{s} = 0.9$, 2.76, 7 and 13 TeV [8, 9] were measured by the CMS detector at the LHC. Such data is limited to the rapidity range $|y| < 1$, the pseudorapidity range $|\eta| < 2.4$ and is available for different high multiplicities. Data can be found in [12, 13] thanks to the HEPData project. Particularly, the momentum distribution (2.5a) was used to fit the value of the parameters a, p_0, α. The fitting was made for minimum bias data on the pions' momentum distribution. The results are summarized in the following table

$\sqrt{s}$ (TeV)	a	p_0	α
0.9	26.64±8.93	2.16±1.07	10.59±3.54
2.76	21.16±5.53	1.39±0.63	7.47±1.90
7	43.65±21.31	3.25±2.00	12.54±5.74
13	15.66±5.35	0.92±0.60	5.54±1.69

Table 1: Values of fitting parameters for different center-of-mass energies.

To avoid resonance effects the fit is restricted to the range $p_T > 0.4$ GeV/c [7]. By using the values p_0, α in Table 1 a new fit is performed for the minimum-bias distribution. A cluster density value ζ is found and a Color Supression Factor and a effective temperature are assigned by equations (2.3) and (2.4) [14]. Similarly for high multiplicities. Nonetheless, for high multiplicity transverse momentum distributions a temperature and Color Suppression Factor is assigned to every multiplicity class distribution at different $\sqrt{s}$.

4. Results

By the method formerly described, the global temperatures and color suppression factors for the minimum-bias were found as a function of $\sqrt{s}$, as shown in Figure (1). The temperature increases as $\sqrt{s}$ does and the opposite is true for the Color Suppression Factor.

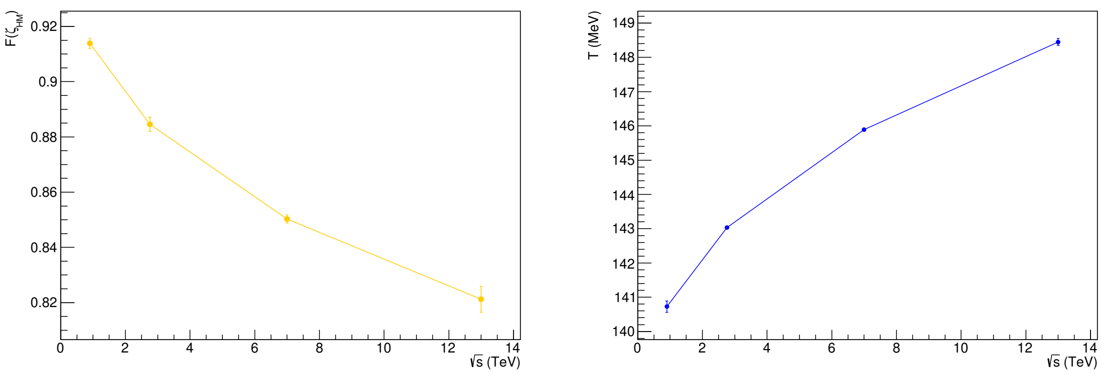

Figure 1: Graphics of $F(\zeta)$ and T as functions of $\sqrt{s}$ for minimum-bias events.

For the high multiplicity case, the second fit is performed several times. Once for every multiplicity class. The secondary results of such fitting, equation (2.6b), are shown in Figure 2. Each line

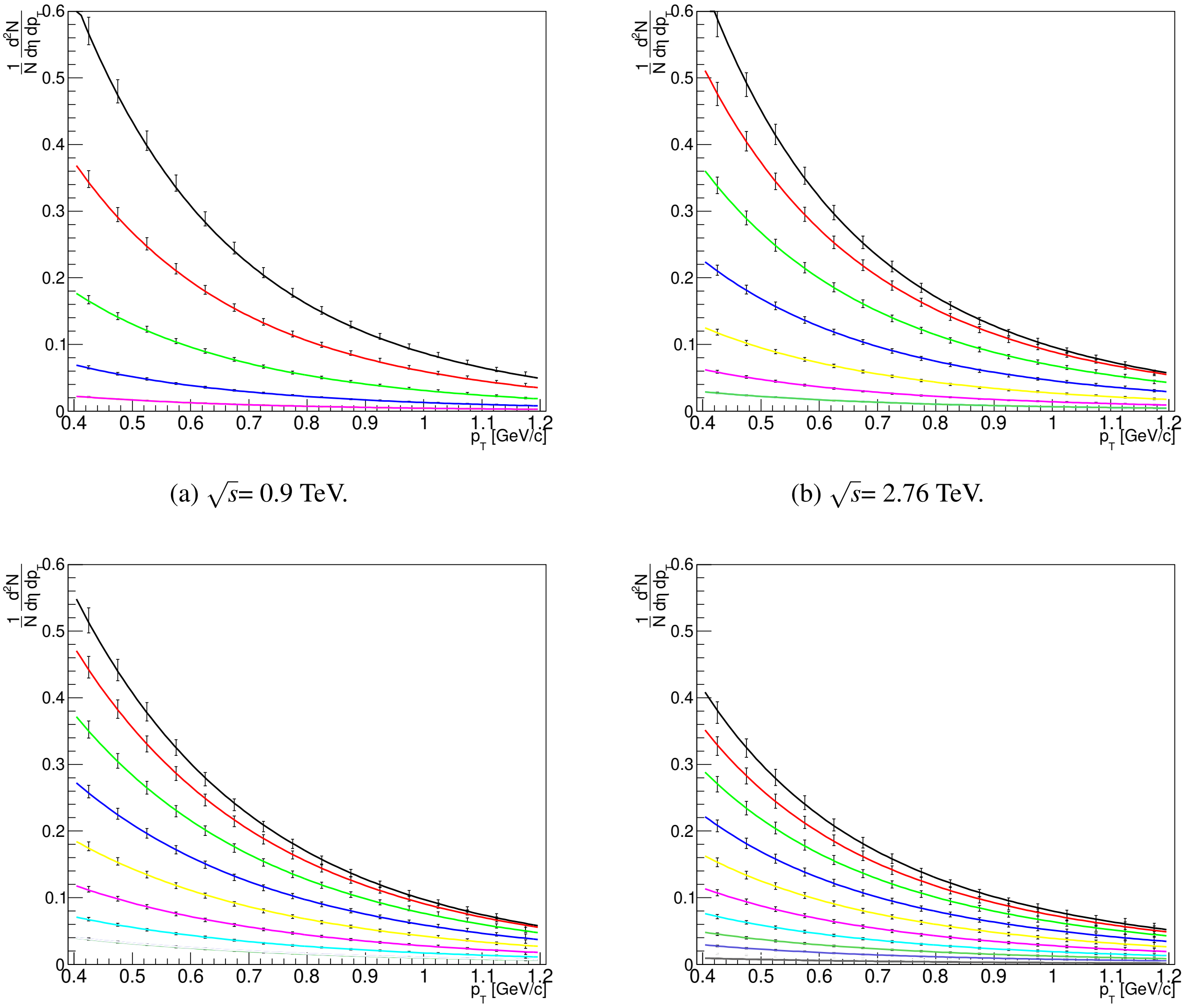

(a) $\sqrt{s}$= 0.9 TeV. (b) $\sqrt{s}$= 2.76 TeV.

(c) $\sqrt{s}$= 7 TeV. (d) $\sqrt{s}$= 13 TeV.

Figure 2: Fitting for different multiplicity classes at $\sqrt{s}$ = 0.9, 2,76, 7 and 13 TeV. Different multiplicity classes were chosen randomly for every $\sqrt{s}$.

in a particular color corresponds to a single multiplicity class. The different values of $\sqrt{s}$ contain several multiplicity classes. The larger $\sqrt{s}$, the wider variety of $\langle N \rangle$.

Given the corresponding ζ, temperatures and $F(\zeta)$ were found for several center-of-mass energies and a wide range of multiplicity classes. The multiplicities 7 and 16 for all energies studied result in a negative density and they do not represent a physical situation. The case of 28 is not a physical case for $\sqrt{s}$ = 7,13 TeV. Negative ζ is the cause behind unphysical situations, for example values of the Color Suppression Factor larger than 1. The point of multiplicity $\langle N \rangle$ = 183 for 13 TeV is not included since the incertitude is large. It is interesting to notice the evolution of the value $F(\zeta_{HM})$ and of the temperature as a function of the multiplicity and is shown in Fig. (3). Not all the multiplicity classes arise in every $\sqrt{s}$ as shown in the same figure. The temperature increases as the multiplicity does and the Color Suppression factor decreases.

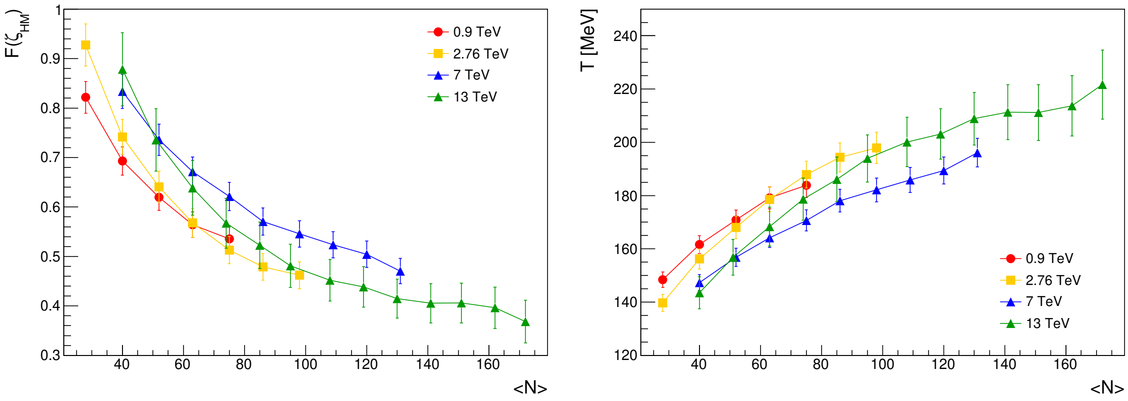

Figure 3: Graphs of $F(\zeta_{HM})$ (right) and T (left) versus multiplicity at $\sqrt{s} = 0.9$, 2.76, 7 and 13 TeV. A universal trend for different $\sqrt{s}$ is observed.

5. Discussion

The results presented for the minimum-bias case show the increasing values of the temperatures and decreasing values of $F(\zeta)$ as $\sqrt{s}$ of the collision increases in Figure (1). Particularly, the Color Suppression Factor behaves asymptotically. In the case of high multiplicity, it is most interesting is to observe the behavior of these quantities for different $\sqrt{s}$. They follow the same pattern and the collision's energy does not seem to affect this trend. The lines crossed each other at some points. Therefore, they follow the same universal trend and the momentum distributions (equations (2.5), (2.6a) and (2.6b)) describe very well the experimental data. It must be mentioned that these ideas of String Percolation Theory in experimental data have been used also in other types of collisions, especially Au-Au collisions at 200 GeV [6]. The results presented are compatible with other types of collisions.

6. Conclusions

The momentum distributions for different $\sqrt{s}$ have a good description by equations equations (2.5), (2.6a) and (2.6b). Values of the Color String Density Parameter decrease and the Temperature increase as the multiplicity $\langle N \rangle$ grows. The values obtained for both the color string density and temperature has a universal trend and the values for high multiplicity are compatible with those obtained for central nucleus-nucleus collisions above 200 GeV.

Acknowledgments

This work could not have been possible without the support of my two tutors: Irais Bautista and Eduardo de la Fuente. I must thank specially Irais and the BUAP since they provided with finantial support throughout the LHCP 2019.

References

[1] H. Satz, *The quark-gluon plasma: A short introduction*, *Nucl. Phys.* **A862-863** (2011) 4 [1101.3937].

[2] K. Christensen, *Percolation theory*, (Imperial College London), (2002), http://web.mit.edu/ceder/publications/Percolation.pdf.

[3] C. Pajares, *String and parton percolation*, *Eur. Phys. J.* **C43** (2005) 9 [hep-ph/0501125].

[4] I. Bautista, J. G. Milhano, C. Pajares and J. Dias de Deus, *Multiplicity in pp and AA collisions: the same power law from energy-momentum constraints in string production*, *Phys. Lett.* **B715** (2012) 230 [1204.1457].

[5] J. Dias de Deus, A. S. Hirsch, C. Pajares, R. P. Scharenberg and B. K. Srivastava, *Clustering of Color Sources and the Shear Viscosity of the QGP in Central A-A Collisions at RHIC and LHC Energies*, 1106.4271.

[6] R. P. Scharenberg, B. K. Srivastava and A. S. Hirsch, *Percolation of Color Sources and the determination of the equation of state of the Quark-Gluon Plasma (QGP) produced in central Au-Au collisions at $\sqrt{s_{NN}} = 200$-GeV*, *Eur. Phys. J.* **C71** (2011) 1510 [1006.3260].

[7] I. Bautista, A. Fernandez Tellez and P. Ghosh, *Collectivity in high-multiplicity events of proton-proton collisions in the framework of String Percolation*, *arXiv e-prints* (2015) [1505.00924].

[8] CMS collaboration, *Study of the inclusive production of charged pions, kaons, and protons in pp collisions at $\sqrt{s} = 0.9$, 2.76, and 7 TeV*, *Eur. Phys. J.* **C72** (2012) 2164 [1207.4724].

[9] CMS collaboration, *Measurement of charged pion, kaon, and proton production in proton-proton collisions at $\sqrt{s} = 13$ TeV*, *Phys. Rev.* **D96** (2017) 112003 [1706.10194].

[10] M. A. Braun, F. Del Moral and C. Pajares, *Percolation of strings and the first RHIC data on multiplicity and transverse momentum distributions*, *Phys. Rev.* **C65** (2002) 024907 [hep-ph/0105263].

[11] B. K. Srivastava, *Percolation and Deconfinement*, *Nucl. Phys.* **A862-863** (2011) 132 [1102.0754].

[12] CMS collaboration, *Study of the inclusive production of charged pions, kaons, and protons in pp collisions at $\sqrt{s} = 0.9$, 2.76, and 7 TeV*, 2012. 10.17182/hepdata.59366.

[13] CMS collaboration, "Measurement of charged pion, kaon, and proton production in proton-proton collisions at sqrt(s) = 13 TeV." https://www.hepdata.net/record/ins1608166, 2017. 10.17182/hepdata.80168.

[14] R. P. S. Brijesh K. Srivastava, A. S. Hirsch and C. Pajares, *De-confinement and percolation in nucleus-nucleus and hadron-hadron collisions*, in *2nd International Workshop on QCD Challenges from pp to AA*, CERN, November, 2017.